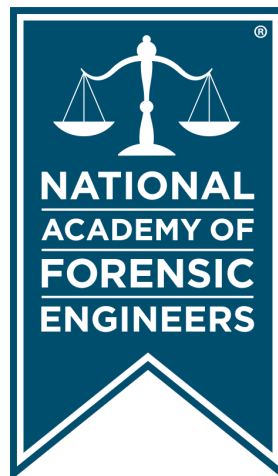


Journal of the  
**National**  
**Academy** OF  
**Forensic**  
**Engineers**<sup>®</sup>



<http://www.nafe.org>

ISSN: 2379-3252

Vol. 37 No. 1 December 2020

# Metallurgical and Mechanical Failure Analysis of an Aftermarket Flywheel

By Nikhil Kar, PhD, PE (NAFE 1095M)

## Abstract

*A failure analysis investigation was performed on the remnants of an aftermarket gray cast iron flywheel that catastrophically fractured during operation in a vehicle after 24 miles of operation. Light microscopy, 3D X-ray micro-computed tomography (micro-CT), scanning electron microscopy (SEM), metallography, and hardness/tensile testing techniques were utilized to characterize manufacturing quality, mode(s) of failure, microstructural variation, fracture surfaces, and mechanical properties of the failed component. Light microscopy examination of the remnant surfaces showed that the flywheel shattered with signs of radial heat checking fissure cracks. A metallurgical examination of the flywheel showed that it was manufactured from cast gray iron, with evidence of microstructural changes near heat-affected zones from graphite flakes in a ferrite/pearlite matrix to needle and lath formations similar to bainite or martensitic phases. The CT scan slices and fracture surface examination in the SEM showed signs of porosity and dendritic formations along a fracture surface believed to be the crack initiation location. The analysis suggests manufacturing flaws found within the flywheel were a likely contributing factor leading to premature failure during service. A review of original equipment manufacturer (OEM) flywheel material specifications showed that the OEM flywheel was manufactured out of ductile nodular iron with significantly higher tensile strength and ductility, an indication that the failed aftermarket flywheel product was not manufactured to meet or exceed OEM specifications.*

## Keywords

Gray cast iron, fissure cracks, porosity, dendrites, manufacturing flaws

## Introduction

Due to ease and low price of manufacturing cast parts, many companies look overseas to various foundries for reverse engineering and aftermarket product development for replacement components that are to be used in classic U.S. muscle cars. This is primarily because U.S. car manufacturers (such as Ford and Chevrolet) no longer support or manufacture OEM parts for these vehicles, and they do not make OEM specifications available (as their designs are considered proprietary and not available to the general public).

Gray cast iron is used in many automotive applications, including camshafts, spring gears, and flywheels. While there are a number of publications related to failure analysis of various vehicle components and flywheels that have been in service for an extended period of time, this paper analyzes the failure of a cast gray iron flywheel that

occurred only after 24 miles, using forensic metallurgical and mechanical techniques including microscopy, metallography, 3D X-ray computed tomography, and scanning electron microscopy.

A review of the literature has shown that Dellinger et al. analyzed a cracked plain carbon steel flex plate from a 1978 Oldsmobile custom cruiser station wagon that had been driven in excess of 200,000 miles and found evidence of a fatigue failure<sup>1</sup>. Becker and Shipley identified microporosity as a major contributing factor in the cracking of a cast gray iron cylinder head<sup>2</sup>. Casting stresses have also been found to cause premature cracking in gray cast iron crank cases<sup>3</sup> due to excessive or rapid cooling during the casting process. Hou and Jiang performed an investigation on an engine crankshaft that suddenly fractured, and they concluded the failure occurred in the ductile iron due to fatigue from bending and twisting with



**Figure 1a**

Overall photograph of fractured flywheel showing side that would mate to crankshaft. Note crankshaft seal outline near center hub.

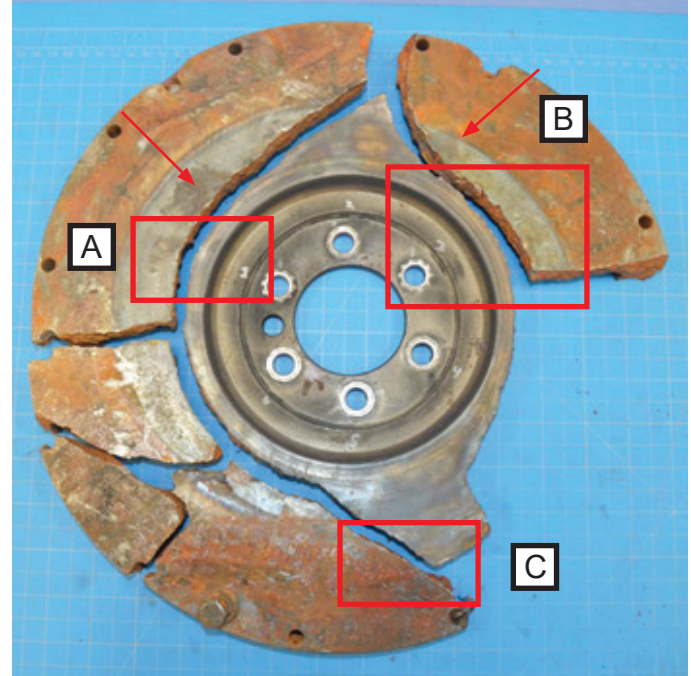


**Figure 1b**

Overall photograph of fractured flywheel showing side that would mate with clutch disk surface. Note heat damage to areas A, B, and C.

cracks originating at subsurface shrinkage<sup>4</sup>. Computed tomography has been used to characterize defects in castings<sup>5</sup>, and has been shown to have excellent sensitivity in revealing casting defects.

## Background

An aftermarket replacement flywheel that was advertised as meeting or exceeding OEM specifications was used in a vehicle conversion from an automatic transmission to a four-speed manual transmission. The transition and installation occurred over a period of a week, and the vehicle was driven for 24 miles prior to catastrophic fracture and failure of the flywheel based on a forensic investigation. The flywheel fractured into multiple components when the vehicle was in neutral, and the engine was being revved to 3,500 rpm for 3 to 5 seconds.

**Figure 1** shows two photos of the remnant portions of the flywheel that were collected after the incident occurred. **Figure 1a** shows the side of the flywheel that would face the crankshaft; **Figure 1b** shows the side that would make contact with the clutch disk when the clutch pedal is disengaged in neutral or in gear. The flywheel was manufactured at an overseas foundry using a casting process with appropriate dimensions for the application and was routinely sold at automotive retailers that provide aftermarket parts to older vehicles when OEM parts are not available.

## Findings

### Fractography

Macroscopic inspection photographs of the fracture surface are shown in **Figure 2** at locations A, B, and C as indicated in **Figure 1**. These surfaces show heat tinting, discoloration, and radial fissure cracks on the side of the flywheel that would make contact with the clutch pad disk. The central portion of the remnant flywheel containing the bolt holes for mounting the flywheel to the crankshaft had a complete circumferential fracture surface that was examined in detail using visual examination, optical microscopy, and scanning electron microscopy techniques. Location C was unique, as it was the only area that contained both radial and circumferential fracture surfaces, as shown in **Figure 2c**.

An end-on photograph of the circumferential fracture surface at location C is shown in **Figure 3a**. The majority of the fracture surface appears dull, with a small band of a shiny fracture surface near the lower left and lower right region. SEM examination in the dull location as shown in **Figure 3b** shows that the dull surface was comprised of dendrites, porosity, and material that was not fractured, but rather it was liquid that solidified and did not fuse with any other material when casting of the flywheel occurred. The figure shows the surface contains dendrites, an indication that this entire surface separated and contained porosity; a



**Figure 2a**

Close-up photomicrograph in location A shows heat tinting and fissure cracks.



**Figure 3a**

End on view of location C shows dull fracture surface.

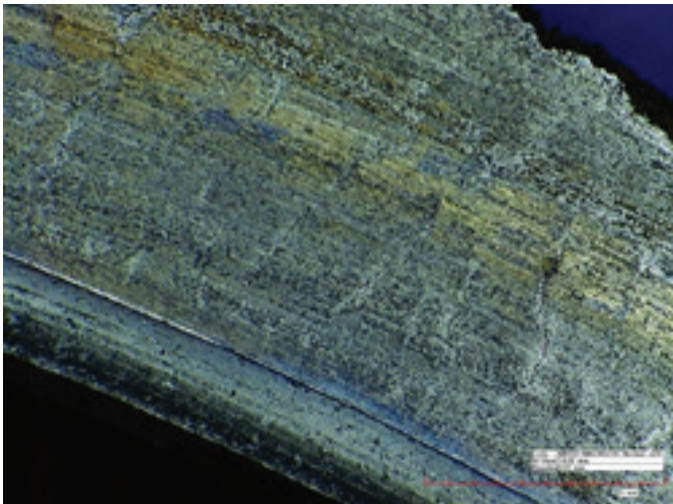


**Figure 2b**

Close-up photomicrograph in location B shows heat tinting and fissure cracks.

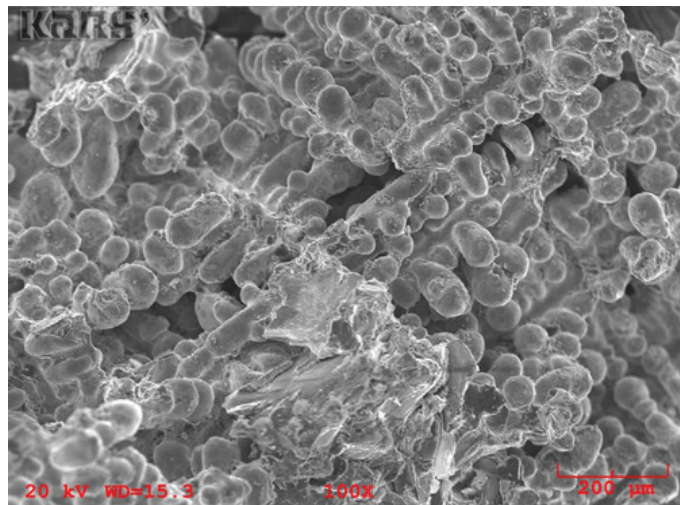


**Figure 3b**

High magnification SEM image in dull fracture surface area shows dendrites and solidified droplets that were not fractured.

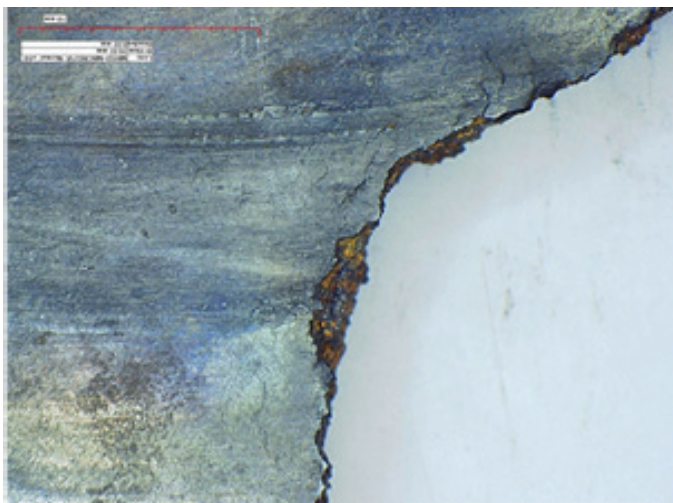


**Figure 2c**

Close up photomicrograph in location C shows heat tinting and fissure cracks.

likely initiation site that led to catastrophic failure of the entire flywheel. While all castings may contain some level of porosity that is generated due to internal gas entrapment and material shrinkage during solidification, it is important to identify and quantify the amount of porosity from a manufacturing quality standpoint.

### Computed Tomography

The location and appearance of porosity and dendrites where fracture initiation occurred was suitable for 3D X-ray computed tomography, as it could be used to understand the distribution and location of the porosity. 3D X-ray computed tomography is a non-destructive inspection technique that uses high-energy X-rays to create thousands of radiographic images of a sample as it rotates about a central axis. A computer algorithm is then used to combine the radiographic images that generate a 3D model that can be sliced in software to reveal internal structural details of

any material.

**Figure 4a** shows the location of area C in the flywheel and the reference CT slice data in **Figure 4b**. **Figure 5**, a magnified CT slice view of area C, indicates that the porosity envelopes the entire width of the fracture surface, which is 1.6 in. in length.

**Figure 6** shows a CT slice transverse view of location C, an indication to the depth of the porosity, which was measured to be 0.4 in. deep. The slices provide information regarding the amount of porosity and proximal location to the fracture surface, which cannot be seen using



**Figure 4a**

Overall view of flywheel remnants and location for computed tomography.

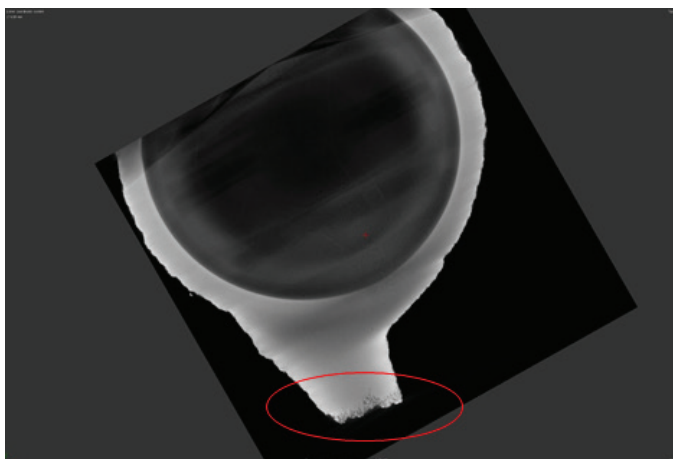


**Figure 4b**

CT slice shows no porosity except near fracture surface as indicated.

visual microscopic techniques. The CT analysis of this area shows casting flaws, and metallography was performed in this area to understand the microstructural differences in the flywheel at such locations.

### Metallography and Microstructure

**Figure 7** contains three photomicrographs obtained from representative areas in the flywheel that characterize the base cast gray iron microstructure, microstructural changes due to heat/temperature exposure, and metallurgical deficiencies due to casting. **Figure 7a** shows that the base microstructure is consistent with gray cast iron, containing graphite flakes in a matrix of ferrite and pearlite grains. **Figure 7b** shows that in the heat-affected zone, the gray cast iron has transformed into different phases of needle and lath type structures similar to bainite or martensite. Metallurgical deficiencies in the form of dendrites



**Figure 5**

High magnification CT slice shows porosity and dendrites along fracture surface location.

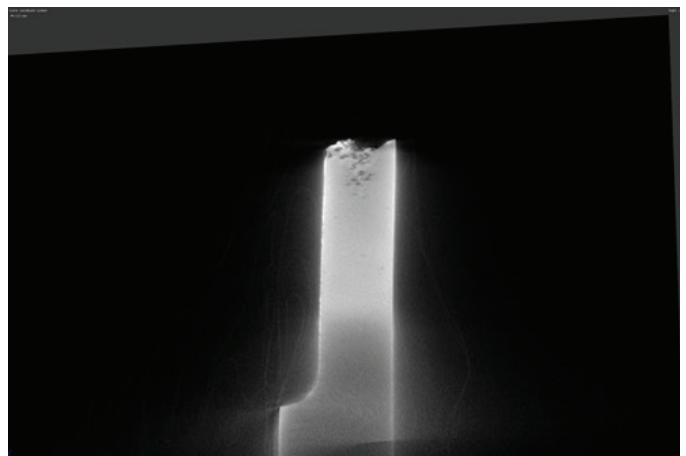


**Figure 6**

High magnification transverse CT slice shows porosity depth and dendrites along fracture surface.

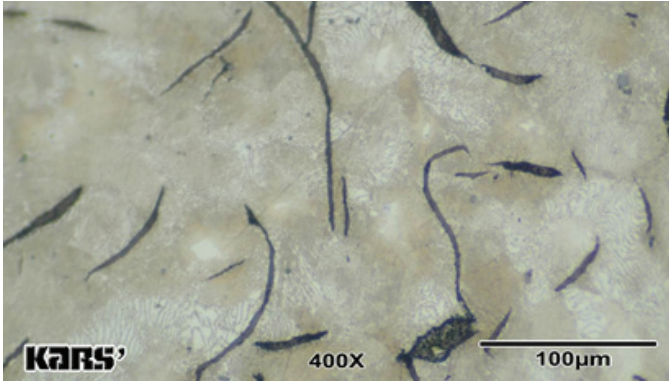


**Figure 7a**

Photomicrograph of base cast gray iron microstructure shows ferrite pearlite matrix with graphite flakes.

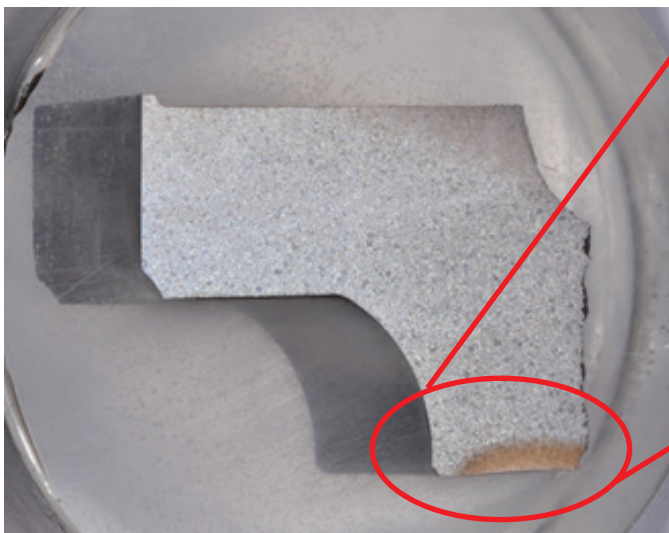


**Figure 7b**

Photomicrograph of heat-affected zone shows fissure cracks and microstructural changes to include needle and lath features similar to bainite or martensite phases. Photomicrograph of base cast gray iron microstructure shows ferrite pearlite matrix with graphite flakes.

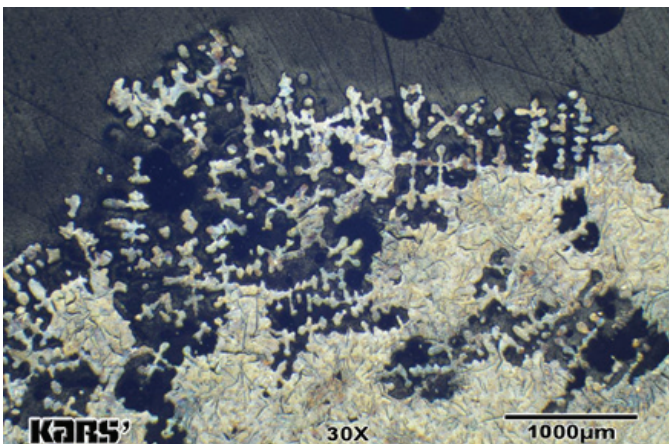


**Figure 7c**

Photomicrograph shows casting porosity and dendrites, indicating poor casting procedures.

and porosity due to rapid solidification and shrinkage during casting are shown in **Figure 7c**. This cross section was taken from area C as discussed in **Figure 3** and **4**. These areas were found on, and within the radial and circumferential fracture surface (Area 3), where it is believed the failure initiated.

### Mechanical Testing

Sub-specimen flat dogbone tensile coupons consistent with ASTM E8 were machined away from the heat-affected zone in the subject flywheel to determine mechanical properties, the results of which are shown in **Figure 8** and **Figure 9**. These results confirm that the material was manufactured from gray cast iron with a tensile strength similar to that of SAE G3500 (35 KSI) and

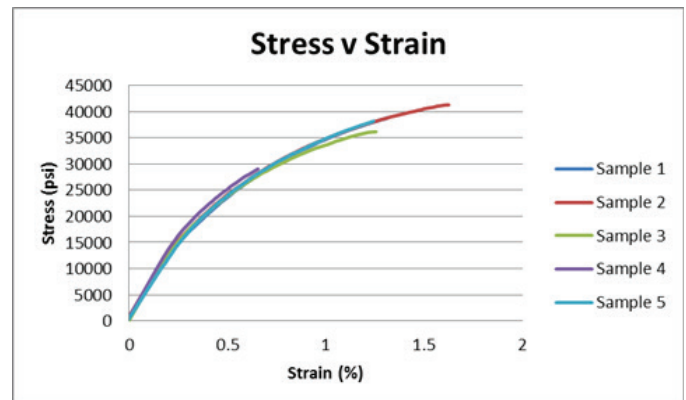
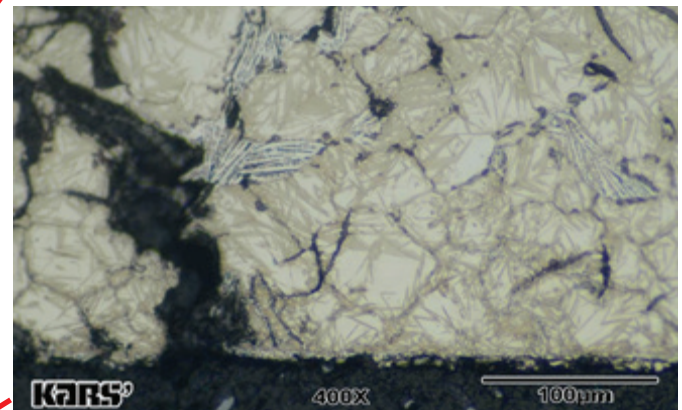


**Figure 8**

Tensile stress versus elongation of five tensile coupons machined from failed flywheel away from heat affected zone.

hardness of 215 HRB. Similar testing was performed on an OEM flywheel, and the testing results showed the OEM flywheel was manufactured out of ASTM A536 ductile iron with a tensile strength of 80 KSI, a yield strength of 55 KSI and an elongation of 6%. Gray cast iron materials are brittle, and — when subject to metallurgical defects — heat and substantive stresses rapid and catastrophic fracture can occur.

Sample	Gage Length (in)	Width (in)	Thickness (in)	Area (in <sup>2</sup> )	Maximum Load (lbf)	UTS (psi)	Elongation at Fracture (%)
1	1	0.1322	0.0644	0.00851368	338.77	39791.25	1.422499958
2	1	0.1272	0.062	0.0078864	325.74	41304.02	1.62499994
3	1	0.1309	0.061	0.0079849	288.73	36159.5	1.25500001
4	1	0.1289	0.063	0.0081207	315.55	38857.49	1.397500001
5	1	0.1339	0.0643	0.00860977	350.1	40663.11	1.489999983
						39355.07	1.437999979

**Figure 9**  
Tabulated stress strain data.

## Discussion

The failure analysis investigation on the fractured flywheel showed three important metallurgical and material factors contributed to the catastrophic failure shortly after installation. Evidence of heat and temperature generated microstructural changes led to the formation of radial surface fissure cracks along a circumferential area where the clutch disk engaged the flywheel.

While the formation of heat check cracks can occur in flywheels, the rapid propagation and growth of the surface generated cracks is more susceptible in cast gray iron flywheels due to its inherent brittle nature due to graphite flakes in the microstructure, low ductility and low toughness. Localized porosity was found along the fracture surface. Rapid propagation and growth of the surface cracks allowed for catastrophic fracture of the flywheel.

Testing data shows that the fractured flywheel did not meet or exceed OEM specifications, lacking sufficient yield strength, had 60% lower tensile strength when compared to the OEM product and had 1% elongation versus 6% elongation of the OEM product. The lack of performance and sub-standard material selection of cast iron grade flywheels is noted in the racing industry, as SFI Foundation Inc. – Quality Assurance Specifications Specification 1.1 indicates no racing flywheel can be manufactured out of cast iron due its low strength, ductility and toughness.

Had the fractured flywheel been adequately designed or manufactured without casting deficiencies, or alternate material selection, it would have been able to resist crack propagation and growth of the heat fissure cracks generated due to clutch engagement. If the failed flywheel were manufactured out of ductile iron like the OEM flywheel, it is likely that a different mode of failure would have occurred where deformation or significant warping of the flywheel would have given the vehicle operators an indication that a failure was occurring, and catastrophic fracture would likely not have occurred.

## Conclusion

An investigation was performed on an aftermarket replacement flywheel that failed after 24 miles of use. The author’s findings suggest significant metallurgical deficiencies in the form of porosity and dendrites contributed to the premature failure of the flywheel when exposed to temperature loading during use. Microstructural changes and heat tinting occurred in the cast gray iron material, and a review of the literature has shown that OEM specifications for this vehicle application call for a ductile nodular iron grade of material.

## References

1. D. Dellinger, “Case C: A Cracked Automobile Flywheel Flex Plate,” Failure Analysis of Engineering Materials, pp 483 – 491, 2002.
2. W. Becker and R Shipley, “Example 1: Cracking in a Gray-Iron Cylinder Head Caused by Microporosity,” in ASM Handbook Volume 11 Failure Analysis and Prevention. ASM International, 2002, pp. 112-113.
3. E. Unterweiser, “Example 11: Cracking in a Gray-Iron Cylinder Blocks Caused by Casting Stresses,” in ASM Handbook Volume 11 Failure Analysis and Prevention. ASM International, 2002, pp. 134-135.
4. X. Hou, Y. Li, and T. Jiang, “Fracture Failure Analysis of Ductile Cast Iron Crankshaft in a Vehicle Engine,” Journal of Failure Analysis and Prevention, vol. 11-1 pp. 10-16, 2011.
5. R. Bossi, J. Cline, E. Costello, and B Knutson, “X-ray Computed Tomography of Castings,” Wright Research and Development Center, Interim Report for Period April 1989- September 1989.

## Acknowledgements

*I acknowledge and thank the technical staff at Kars’ Advanced Materials, Inc. for their discussions and assistance.*